Changes of myoid and endothelial cells in the peritubular wall during contraction of the seminiferous tubule

Antonella D. Losinno, Viviana Sorrivas, Marcelo Ezquer, Fernando Ezquer, Luis A. López & Alfonsina Morales

Cell and Tissue Research

ISSN 0302-766X

Cell Tissue Res
DOI 10.1007/s00441-016-2386-x

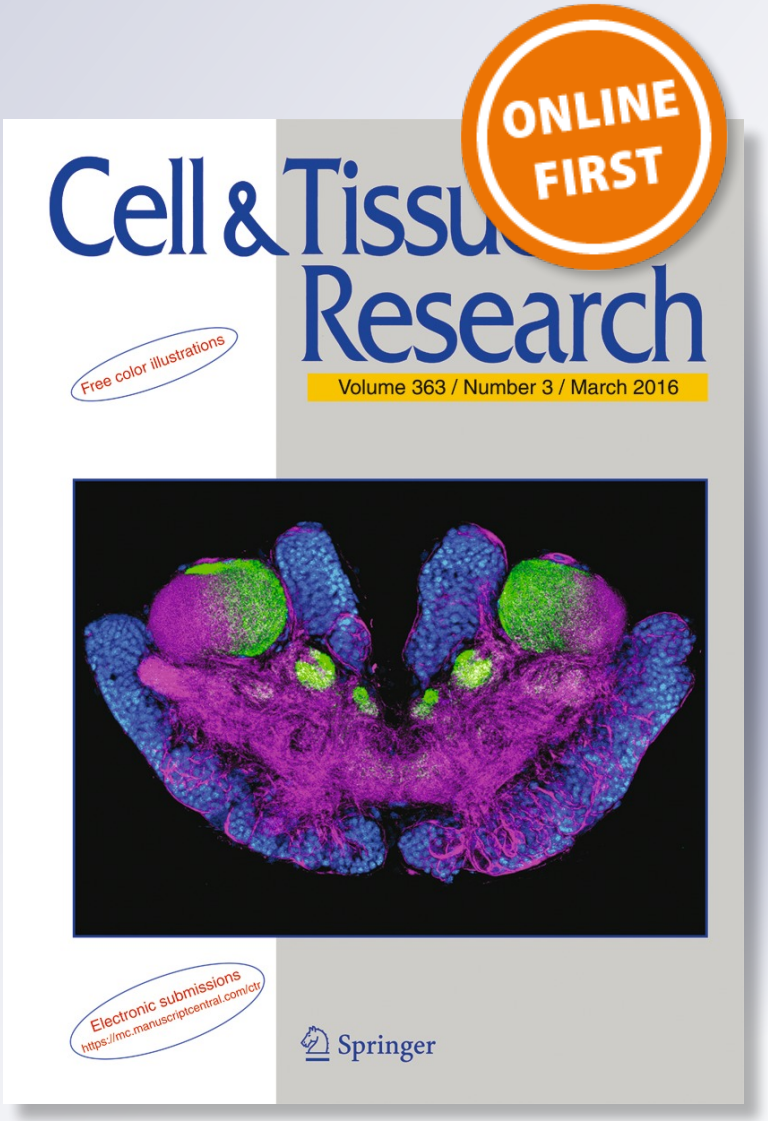

Springer

Your article is protected by copyright and all rights are held exclusively by Springer-Verlag Berlin Heidelberg. This e-offprint is for personal use only and shall not be self-archived in electronic repositories. If you wish to self-archive your article, please use the accepted manuscript version for posting on your own website. You may further deposit the accepted manuscript version in any repository, provided it is only made publicly available 12 months after official publication or later and provided acknowledgement is given to the original source of publication and a link is inserted to the published article on Springer's website. The link must be accompanied by the following text: "The final publication is available at link.springer.com".

Author's personal copy

Cell Tissue Res
DOI 10.1007/s00441-016-2386-x

REGULAR ARTICLE

Changes of myoid and endothelial cells in the peritubular wall during contraction of the seminiferous tubule

Antonella D. Losinno[1] · **Viviana Sorrivas**[2] · **Marcelo Ezquer**[3] · **Fernando Ezquer**[3] · **Luis A. López**[1] · **Alfonsina Morales**[1]

Received: 23 October 2015 / Accepted: 19 February 2016
© Springer-Verlag Berlin Heidelberg 2016

Abstract The wall of the seminiferous tubule in rodents consists of an inner layer of myoid cells covered by an outer layer of endothelial cells. Myoid cells are a type of smooth muscle cell containing α-actin filaments arranged in two independent layers that contract when stimulated by endothelin-1. The irregular surface relief of the tubular wall is often considered a hallmark of contraction induced by a variety of stimuli. We examine morphological changes of the rat seminiferous tubule wall during contraction by a combination of light, confocal, transmission and scanning electron microscopy. During ET-1-induced contraction, myoid cells changed from a flat to a conical shape, but their actin filaments remained in independent layers. As a consequence of myoid cell contraction, the basement membrane became wavy, orientation of collagen fibers in the extracellular matrix was altered and the endothelial cell layer became folded. To observe the basement of the myoid cell cone, the endothelial cell monolayer was removed by collagenase digestion prior to SEM study. In contracted tubules, it is possible to distinguish cell relief: myoid cells have large folds on the external surface oriented parallel to the tubular axis, whereas endothelial cells have numerous cytoplasmic projections facing the interstitium. The myoid cell cytoskeleton is unusual in that the actin filaments are arranged in two orthogonal layers, which adopt differing shapes during contraction with myoid cells becoming cone-shaped. This arrangement impacts on other components of the seminiferous tubule wall and affects the propulsion of the tubular contents to the rete testis.

Keywords Seminiferous tubules · Endothelin-1 · Testis ultrastructure · Peritubular myoid cell · Alpha-actin

Introduction

The seminiferous tubules (ST) of the adult rodent testis are surrounded by a wall (boundary tissue) consisting of a continuous monolayer of peritubular myoid cells (MC) (Vogl et al. 1985; Palombi et al. 1992). This wall is in turn covered by a monolayer of endothelial cells (EC) that faces the interstitium (Fawcett et al. 1969; Clark 1976; Yazama et al. 1997; Söderström 2009). Each of these monolayers is easily identifiable by transmission electron microscopy (TEM).

Both MC and EC are mononuclear cells with a polygonal shape. MC are a specialized type of smooth muscle cells. Like other types, they are contractile cells that express cytoskeletal markers, including α-isoactin, desmin and smooth muscle myosin (Virtanen et al. 1986; Tung and Fritz 1990; Fernández et al. 2008). Contractile activity of MC propels spermatozoa and testicular fluid to the rete testis (Tung and Fritz 1990).

MC from rat ST have a cytoskeleton characterized by a complex arrangement of actin and myosin proteins distinct from that present in "typical" smooth muscle cells. We previously demonstrated (Losinno et al. 2012) by confocal

Electronic supplementary material The online version of this article (doi:10.1007/s00441-016-2386-x) contains supplementary material, which is available to authorized users.

✉ Alfonsina Morales
alfonsina_morales2@yahoo.com.ar

[1] Instituto de Histología y Embriología Dr. Mario H Burgos – CONICET. Facultad de Ciencias Médicas, Universidad Nacional de Cuyo, Cuyo, Argentina

[2] Laboratorio de Microscopía Electrónica de la UAT-CCT. CONICET, Bahía Blanca, Argentina

[3] Centro de Medicina Regenerativa, Facultad de Medicina, Clínica Alemana-Universidad del Desarrollo, Santiago, Chile

Published online: 18 March 2016

Author's personal copy

microscopy and TEM that actin filaments (AF) and myosin filaments in MC are arranged in thick bundles distributed as two independent layers within the cell, with no interweaving between the two layers. Each layer consists of parallel filaments arranged orthogonally relative to the other layer (Losinno et al. 2012). Because of this arrangement, MC have (1) an inner circular layer with AF perpendicular to the tubular axis, located in the cytoplasm between the nucleus and the inner surface that faces the tubular side and (2) an outer longitudinal layer with AF parallel to the tubular axis, located between the nucleus and the external surface that faces the interstitium.

The AF bundles of the inner circular layer correspond to those of neighboring cells, forming a cylindrical sheath that tightly surrounds the ST. The AF bundles of the outer longitudinal layer also correspond to those of neighboring cells but form ribbons that run along the ST. Other AF bundles form a peripheral belt in MC that is involved in adherent junctions between the cells (Losinno et al. 2012). Endothelin-1 (ET-1), a peptide synthesized by Sertoli cells in the testis, acts on MC to induce contraction of the ST (Filippini et al. 1993; Nixon et al. 1994; Tripiciano et al. 1996, 1997).

In view of our finding that AF are organized in two independent layers within MC (Losinno et al. 2012) and that the MC sheet is closely associated with the EC sheet, we examined the response of the entire rat ST wall to ET-1 stimulus. For this purpose, we integrated findings from (1) light microscopy and TEM of cross-sections of ST walls, (2) confocal microscopy of cytoskeletal arrangement and (3) scanning electron microscopy (SEM) of MC and EC surfaces.

SEM allows us to view details of EC in the external surface of the ST wall but not the shape of MC in the underlying sheet. To overcome this problem, we established collagenase digestion conditions that allowed us to remove EC from the ST wall and thereby view MC. Our comprehensive SEM studies revealed surface changes of MC and EC under both relaxation and ET-1-induced contraction.

Materials and methods

Animals, reagents and preparation of ST

Wistar rats were born and maintained in our animal colony (12L:12D cycle, food and water ad libitum) and killed at age 3 months in a CO_2 chamber. Animals from different litters were used for each experiment. Animals were maintained in accordance with the National Institutes of Health Guide for the Care and Use of Laboratory Animals. All procedures were approved by the Animal Research Committee of the Universidad Nacional de Cuyo (CICUAL; Protocol approval No. 13/2012).

All reagents were from Sigma-Aldrich (St. Louis, MO, USA) unless stated otherwise.

Testes were removed and decapsulated and ST were carefully teased apart with fine needles and stored in DMEM/F12 medium at 37 °C.

ET-1-induced contraction of ST

ST were treated with 50 nM human ET-1 (Filippini et al. 1993; Fernández et al. 2008) in DMEM/F12 for 5 min at 37 °C. Contraction was confirmed using a stereomicroscope (model SMZ10; Nikon, Tokyo, Japan).

Transmission electron microscopy (TEM)

One set of 50 relaxed ST segments and one set of 50 ET-1-contracted segments were fixed in 5 % glutaraldehyde (Pelco International, CA, USA) in 0.1 M sodium cacodylate buffer for 20 min at 37 °C and then for 2 h at 10 °C in the same buffer. Each set was washed in the same buffer, post-fixed in 1 % OsO_4 for 1 h at room temperature, dehydrated in a graded acetone series and embedded in low-viscosity epoxy resin (Pelco International) as described previously (Spurr 1969). Polymerization was performed for 48 h at 70 °C. Ultrathin sections with interference color gray were cut by an ultramicrotome (Ultracut R; Leica, Wien, Austria), mounted on grids and stained with uranyl acetate and lead citrate (Reynolds 1963). Grids were examined by TEM (model 900; Zeiss, Jena, Germany).

Light microscopy

Thin sections (1 μm thickness) were cut by an ultramicrotome as above, mounted on slides, stained with toluidine blue and observed by light microscopy (model 80i; Nikon). Digital photographs were taken of ST cross-sections.

Immunostaining and confocal microscopy

For each experiment, sets (100 each) of relaxed and contracted ST segments were fixed with 4 % paraformaldehyde in PBS for 20 min at 37 °C, washed with PBS for 10 min 3×, incubated in 50 mM ammonium chloride in PBS for 30 min, rinsed with 0.05 % saponin and 0.2 % BSA in PBS (wash solution) for 10 min 3× and incubated overnight at 4 °C with primary antibody (Ab). The Abs used were anti-α-actin mAb conjugated with FITC ("α-actin Ab") (Sigma; dilution 1:500) and anti-β-actin mAb ("β-actin Ab") (Sigma; dilution 1:500). Samples were rinsed with wash solution for 10 min 3×. ST segments incubated with β-actin Ab were developed with Cy3-conjugated anti-mouse IgG (secondary Ab) (Jackson Immuno Research, PA, USA; dilution 1:200) and rinsed with wash solution.

Author's personal copy

For double-staining assays (α-actin and β-actin), ST segments were sequentially incubated with β-actin Ab, secondary Ab, β-actin Ab again (to block free Fab regions of the secondary Ab), rinsed with wash solution and incubated with α-actin Ab.

Immunostained samples were embedded in NP-gallate mounting medium, coverslipped and examined by confocal microscopy (model FV 1000; Olympus, Tokyo, Japan) with a Paplon ×60 lens.

Appropriate negative controls were included to ensure that the staining observed was specific (see Electronic Supplementary Material, Figs. S1 and S2).

To obtain a *z*-stack, serial optical sections (OS) were taken throughout the depth of the ST segment with step size 200 nm. The first OS was taken at the deepest level of MC (near the germinal epithelium), when the first filament image was detected. Subsequent serial OS were taken until the last filament image was detected at the most superficial level of MC or EC (near the interstitium) (see Electronic Supplementary Material, Captions.)

Morphological parameters

Diameters of relaxed and contracted ST segments (30 each) from three different animals were measured in stereomicroscope images using ImageJ software (Rasband 1997–2006).

Cellular areas of MC and EC in 150 cells per animal, from three different animals, were measured in tangential confocal images of ST segments stained with α-actin Ab and β-actin Ab, respectively, using ImageJ software.

Collagenase digestion

ST from decapsulated testes were dispersed in DMEM/F12 at 37 °C in a Petri dish and incubated in the same medium with and without 0.5 mg/ml collagenase from *Clostridium histolyticum* (release of physiologically active rat hepatocytes tested, Type IV, 0.5–5.0 FALGPA units/mg solid, ≥125 CDU/mg solid) for 5 min with gentle shaking. Following collagenase digestion, samples were rinsed 3× in DMEM/F12 and subjected to SEM study as below (see Electronic Supplementary Material, Digestion "Optimization of digestion conditions for removal of EC monolayer"; Fig. S3 and Video S1–3.)

Scanning electron microscopy (SEM)

ST segments were digested with collagenase or not digested (control). Within each of these two groups, subgroups were contracted with ET-1 or not contracted (relaxed).

ST segments in each of the four resulting groups were fixed in 5 % glutaraldehyde (Pelco International) in 0.1 M sodium cacodylate buffer for 20 min at 37 °C and then for 2 h at 10 °C, washed in the same buffer, dehydrated in a graded series of acetone concentrations, dried by CO_2 critical point drying, mounted on stubs, sputter-coated with gold and examined by SEM (model EVO 40 VP; Zeiss).

Statistical analysis

Data were expressed as mean ± SE. Statistical significance was assessed using Student's *t* test (PRISM v.3.03; GraphPad software). Differences with $p < 0.05$ were considered significant.

Results

ET-1 treatment reduces rat ST diameter

ST diameters under relaxation and under ET-1-induced contraction were measured using a stereomicroscope. Diameters were 315 ± 3 μm for relaxed ST and 187 ± 5 μm for contracted ST ($p < 0.05$). We concluded that ET-1 treatment induced ST contraction under our experimental conditions (Fig. 1).

Morphology of MC and EC under relaxation and contraction was evaluated by toluidine blue staining of ST cross-sections using light microscopy. EC were easily distinguished from MC even though both are thin, flattened cell types. In relaxed ST, the EC surface facing the interstitium was smooth (Fig. 2a, c). In contracted ST, MC were thick and protruded into the tubular epithelium, EC had small cytoplasmic projections facing the interstitium and both MC and EC had folded nuclei (Fig. 2b, d).

TEM observation of wall ultrastructure in relaxed and contracted rat ST

ST are surrounded by a continuous double monolayer of cells (Fig. 3). The inner monolayer consists of MC. The outer layer consists of EC and faces the interstitium. Ultrathin sections were taken of ST under relaxation and contraction and wall ultrastructure was analyzed by TEM.

Structures observed in sequence, from the ST external surface to the interstitium, were the basement membrane of the germinal epithelium, an inner space with collagen fibers, the MC monolayer with its inner and outer basement membranes, an outer space with collagen fibers and the EC monolayer.

The basement membrane of the germinal epithelium was continuous and delicate. In the MC monolayer, the inner basement membrane was amorphous and discontinuous, whereas the outer one was thicker and continuous (Fig. 3c, d).

The MC of relaxed ST, looked very flat, contained AF arranged in an inner circular layer and an outer longitudinal layer, with bundles perpendicular and parallel to the tubular

Author's personal copy

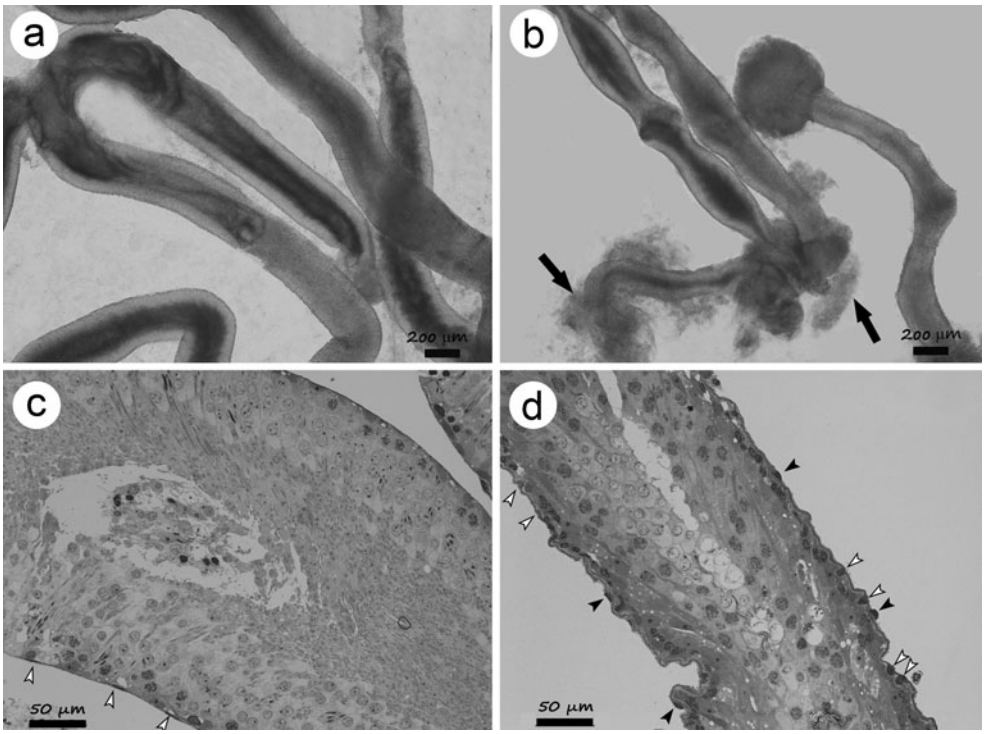

Fig. 1 Relaxed and contracted ST observed by light and stereomicroscopy. Whole unfixed ST observed by stereomicroscopy **a** before and **b** after ET-1 treatment. ET-1 reduces ST diameter in ~40 % and produces the expulsion of ST content from their extremes (*arrow*). Longitudinal sections of **c** relaxed and **d** contracted ST stained with toluidine blue and observed by light microscopy, showing MC (*white arrowheads*) and EC (*black arrowheads*) profiles with respect to the tubular thickness

axis, respectively (Fig. 3a, c). These two layers ran independently with no interweaving and had a cytoplasmic space between them in which the nucleus, rough endoplasmic reticulum and mitochondria were located. EC were relatively thin and contained no AF bundles. Both MC and EC had plasma membranes with smooth surfaces and numerous caveolae.

In contracted ST, MC were convex toward the tubular epithelium, nuclei were folded and heterochromatin was present under the nuclear membrane (Fig. 3b, d). Basement membranes of both epithelium and MC were markedly wavy (Figs. 3d, 4a–d). The orientation of collagen fibers was altered, becoming frequently perpendicular to basement membranes (Fig. 4b, d).

Numerous caveolae were present on the surfaces of MC and EC under both contracted and relaxed conditions (Figs. 3d, 4a, c). Plasma membrane surfaces of both cell types were irregular. EC projections to the interstitium were abundant and small (Figs. 3b, 4a, b).

These findings demonstrate that MC contraction causes altered arrangement of several components of the ST wall, including basement membranes, collagen fibers and the EC monolayer.

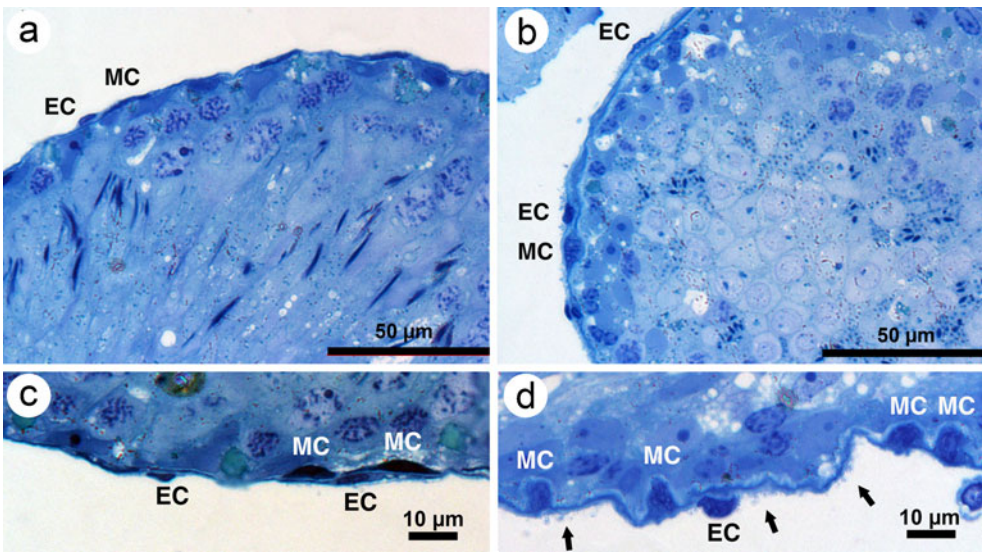

Fig. 2 ST cross-sections stained with toluidine blue and observed by light microscopy. **a** Relaxed ST. The thin wall consists of myoid cells (*MC*) that face the germinal epithelium and endothelial cells (*EC*) that face the interstitium. MC and EC both have a flat shape. **b** Contracted ST. MC and EC both have folded nuclei. MC protrude into the epithelium. **c** Relaxed ST, showing the smooth surface of the wall. **d**. Contracted ST, showing detail of the numerous cytoplasmic projections (*arrows*) of EC into the interstitium

Author's personal copy

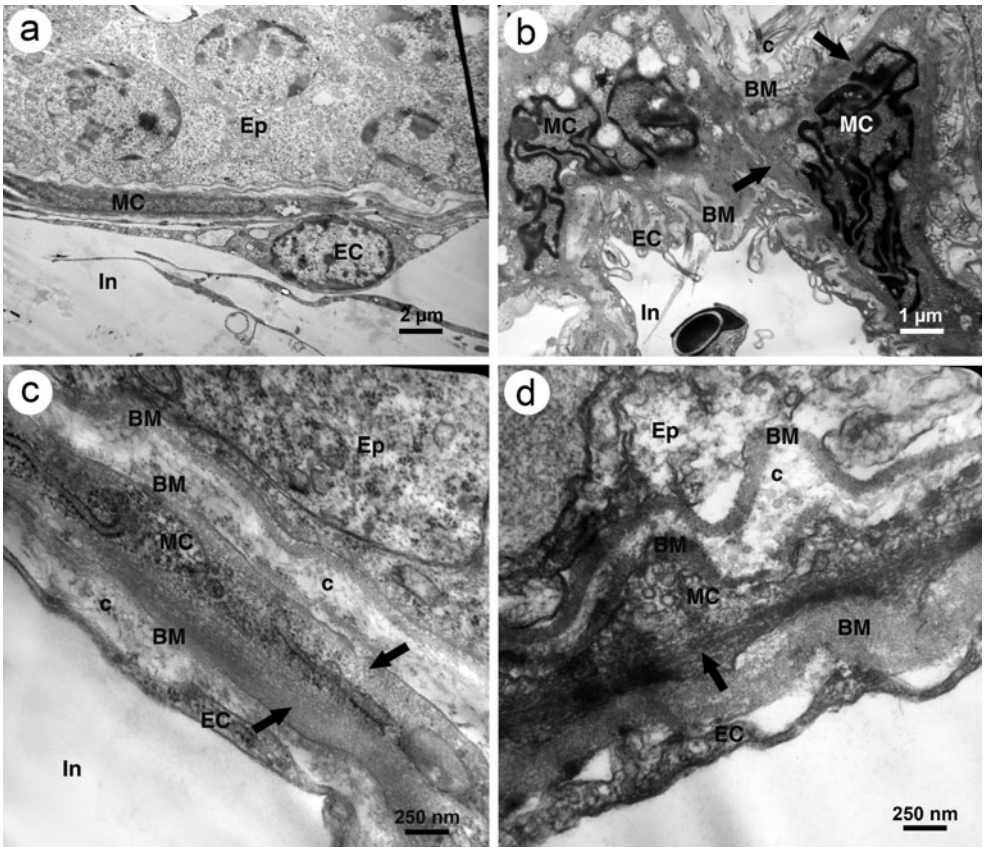

Fig. 3 TEM images of relaxed versus contracted ST. **a** Relaxed ST, showing germinal epithelium (*Ep*) covered by MC and EC monolayers. **b** Contracted ST, showing folded MC and wavy basement membranes (*BM*). MC maintain two independent layers above and below their nuclei (*arrows*). EC have cytoplasmic projections (*arrowheads*) into the interstitium (*In*). **c** Relaxed ST, showing detail of tubular wall. MC, between Ep and EC, have AF arranged in two independent layers (*arrows*), oriented in orthogonal directions. **d** Contracted ST, showing detail of tubular wall. AF from one of the layers (*arrow*) inside MC form a thicker and more interwoven sheet than in relaxed ST. Wavy BM, caveolae of EC and MC and collagen fibers in (**c**) are visible

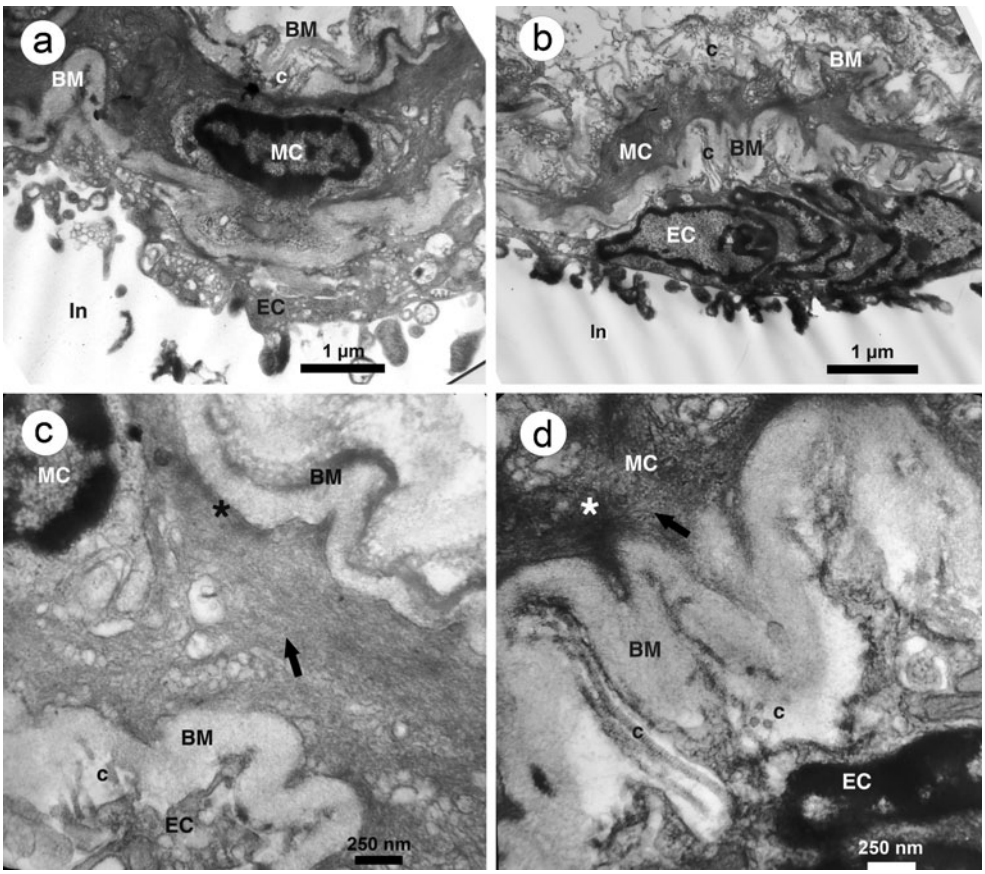

Fig. 4 TEM images of wall morphology of contracted ST. **a**, **b** Basement membranes (*BM*) are highly folded. Collagen fibers *c* are present between germinal epithelium and inner BM of MC and between outer BM of MC and EC. Outer BM of MC is very thick. EC have an irregular surface with cytoplasmic projections into the interstitium (*In*). **c** Detail from (**a**) showing organization of AF (*arrow*) in MC. The AF are more interwoven than in relaxed ST, with intermittent, dense anchorages to the cytoplasmic membrane (*asterisk*). Numerous caveolae in MC and EC are visible. **d** Detail from (**b**) showing arrangement of collagen fibers *c* between the outer BM of MC and EC

Author's personal copy

Change from flat to conical shape and retaining of two independent AF layers in contracted MC of rat ST

Immunostaining of α-actin was used to study MC cytoskeletal arrangements in relaxed and contracted ST, since MC are the only cells in ST that express this protein.

Confocal microscopy showed that MC in relaxed ST were large and polygonal, forming a continuous "tiled floor" (Fig. 5). MC had a peripheral AF "belt" that outlined their contour. MC surface area was 1819.4 ± 68.8 μm^2. In contracted ST, compared with relaxed ST, MC were smaller and more rounded, the peripheral AF "belt" was thicker and the MC surface area at the outer tangential surface was 1127.0 ± 77.9 μm^2 (Fig. 5).

To scan AF throughout the thickness of the MC, we applied the *z*-stack function from the deepest to the most external OS. In the deepest OS of relaxed ST, AF were oriented perpendicular to the tubular axis. In the external OS, AF were oriented along the tubular axis. Thus, the cytoskeleton was organized in two flat layers: an inner circular layer and an outer longitudinal layer (Fig. 6; Electronic Supplementary Material Video S4). The AF from both layers corresponded with the adjacent cells, forming continuous sheaths that are tight round ST in transverse and longitudinal directions.

In contracted ST, AF of the inner circular layer in the deepest OS were also oriented perpendicular to the tubular axis but appeared as isolated groups (Fig. 6; Electronic Supplementary Material, Video S5). In the external OS, the outer longitudinal layer appeared as a single plane, forming dense ribbons running along the ST, upon cellular nuclei. These ribbons corresponded to those of adjacent MC but were more tightly packed than in relaxed ST. These findings indicate that MC in contracted ST change from a flat to a conical shape, with evident changes in the aspect of their two AF layers. The inner circular layer of AF has a convex surface with the top facing the germinal epithelium, while the outer longitudinal layer forms the flat base of the cone. The area of the cone base for contracted MC is less than the outer area of relaxed MC.

EC constitute a continuous monolayer that covers MC in rats

To evaluate coverage of the MC monolayer by the EC monolayer, we immunostained ST segments with both α-actin and β-actin Abs. Moving from the MC level (positive α-actin staining) to the most external OS of the ST wall, we found AF of EC stained with anti β-actin antibody (Fig. 7) forming a continuous sheet over the MC monolayer. The AF of EC did not show defined bundles as observed in MC and were more homogeneously distributed in the cytoplasm. Due to AF not being organized in the peripheral belt, the contours of EC were not well defined. The tangential area occupied by EC in relaxed ST was measured as 3751.5 ± 805.3 μm^2. We were not able to measure the EC tangential area in contracted ST.

These findings indicate that EC constitute a monolayer (sheet) of flat, heterogeneously-sized polygonal cells that completely covers the MC monolayer.

Contraction alters surface relief of MC and EC monolayers

Changes in surface relief of the ST wall are considered a hallmark of contraction. We observed EC and MC surfaces of relaxed and contracted ST by SEM.

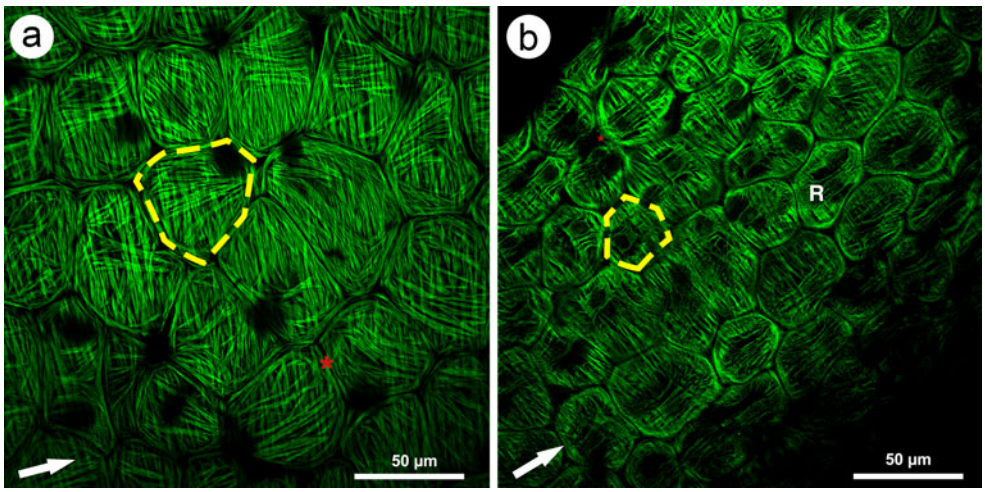

Fig. 5 Confocal microscopic images of MC in **a** relaxed and **b** contracted ST. ST segments were incubated with α-actin Ab. *Dashed lines*: MC contour. MC in contracted ST (**b**) occupy less area and have a more rounded shape compared with those in relaxed ST (**a**). In both relaxed and contracted ST, (1) MC have peripheral belts (*asterisk*) of AF that delimit their contour and (2) AF are arranged in two directions: parallel and perpendicular to the ST tubular axis (*arrow*). In contracted ST (**b**), the AF running parallel to the axis are grouped to form ribbons (*R*)

Author's personal copy

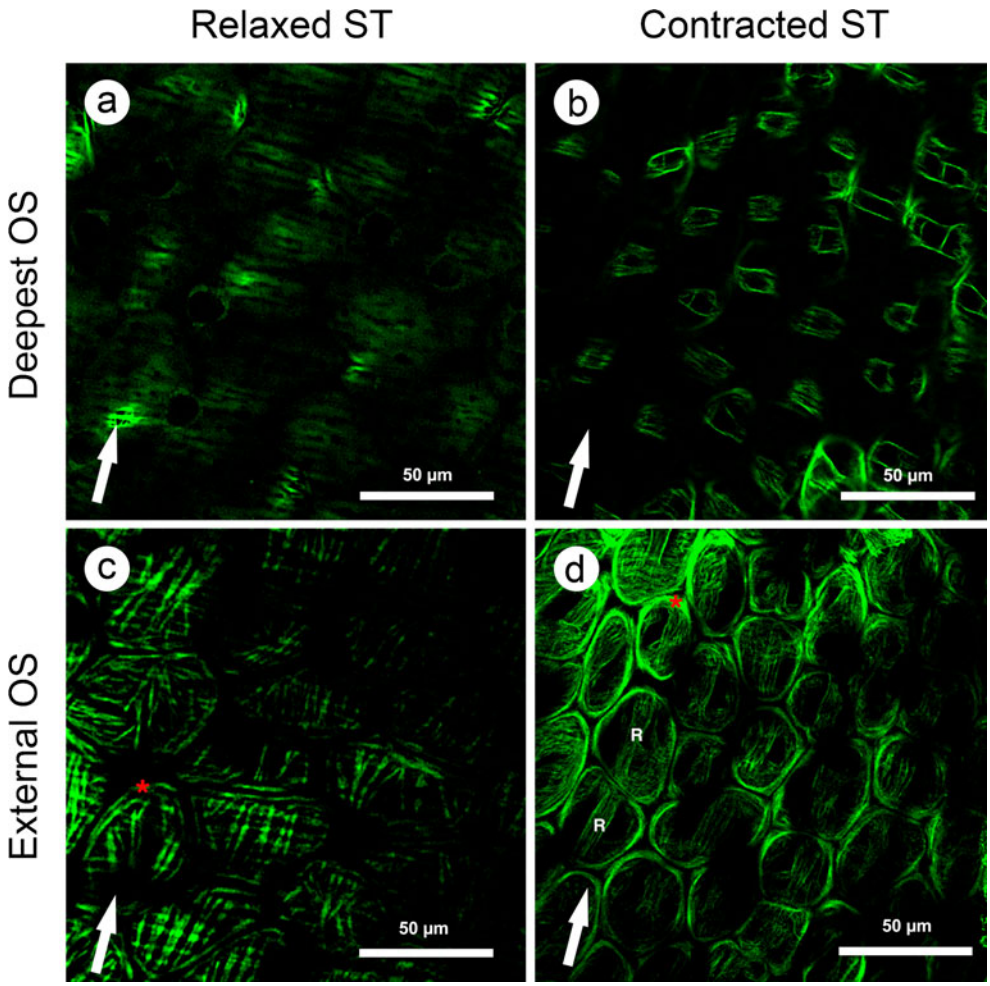

Fig. 6 Confocal microscopic images of deepest and external optical sections (*OS*) of MC from relaxed versus contracted ST. ST were incubated with α-actin Ab and walls were examined sequentially from the germinal epithelium (*Deepest OS*) to the interstitium (*External OS*). In relaxed ST, AF in MC were homogeneously distributed, perpendicular to the ST axis (*arrow*) in deepest OS (**a**) and parallel to the axis in external OS (**c**), corresponding, respectively, to the inner circular layer and outer longitudinal layer. In contracted ST, AF of the inner circular layer appear as small isolated groups in deepest OS (**b**), whereas AF of the outer longitudinal layer form dense ribbons (*R*) running along ST in external OS (**d**). Peripheral AF belts (*asterisk*) are thicker than in relaxed ST

Relaxed ST surface

Non-digested ST segments were always covered by the EC monolayer (Fig. 8a, b). Flat, polygonal EC had a smooth surface and overlapped MC. Nuclei of both EC and MC protrude into the interstitium. EC had a border of intercellular junctions (Fig. 8b, *arrow*) in the periphery. Because they were so thin, some MC contours could be perceived below them (Fig. 8b, *arrowheads*). In digested ST (Fig. 8c, d), the EC monolayer was removed from much of the ST wall to reveal MC, although EC "patches" remained in some areas. MC had a smooth surface with some adhered collagen fibers.

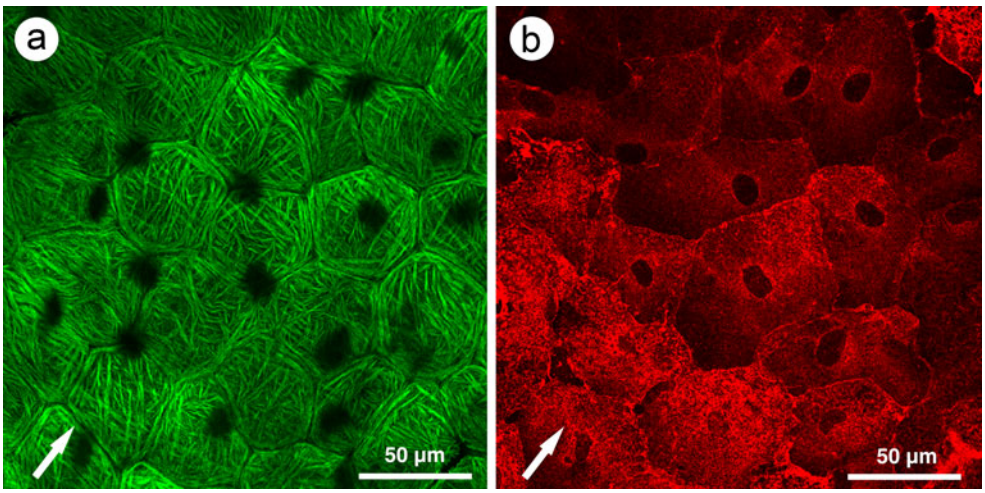

Fig. 7 Confocal microscopic images of MC and EC from relaxed ST. Images were obtained from the same optical field **a** at the MC level (α-actin Ab positive; *green*) and **b** at the EC level (β-actin Ab positive; *red*). MC and EC both have polygonal shape. β-Actin in EC (**b**) does not form defined bundles (in contrast to α-actin in MC) and does not form a peripheral belt around EC. *Arrow* ST axis

Author's personal copy

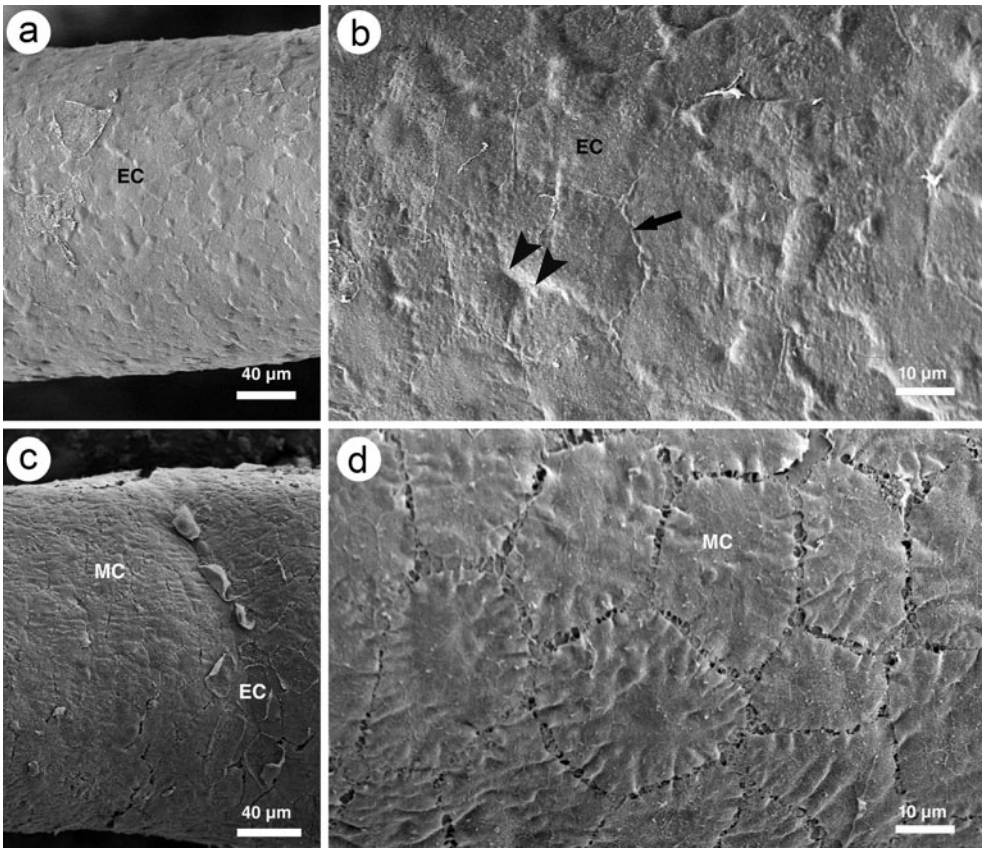

Fig. 8 SEM images of MC and EC monolayer surfaces in relaxed ST. **a** Without collagenase digestion; EC monolayer is present. **b** Higher magnification of the ST segment in (**a**), showing the smooth surface and intercellular junctions (*arrow*) of EC. Some MC boundaries are visible under the EC monolayer (*arrowheads*). **c** The EC monolayer has been mostly removed by digestion. The MC monolayer is exposed, although a few EC are still present. **d** Higher magnification of the ST segment in (**c**), showing the smooth surface of MC. The small spaces among MC are a technical artifact

Contracted ST surface Non-digested ST segments contracted by ET-1 treatment had numerous small projections on EC surfaces. Nuclei were evident but boundaries between cells were not visible among the projections (Fig. 9a, b). Digested ST segments contracted by ET-1 had MC among the EC patches (Fig. 9c, d). The MC surface had large folds running along the tubular axis and small folds perpendicular to the large ones (Fig. 9d, *large and small arrows*). It was not possible to perceive MC contours among the numerous folds. The surface relief of EC, with small, non-oriented, finger-like projections, was easily distinguished from that of MC, with large folds running along the tubular axis of ST.

Discussion

The wall of rodent ST is composed of a continuous cellular sheet made up of flat EC, outside another sheet made up of MC. The EC of ST have been described previously as mesenchymal cells (Leeson and Leeson 1963; Leeson and Forman 1981), fibroblasts (Ross 1967; Kormano and Hovatta 1972) and EC from lymphatic vessels (Fawcett et al. 1969; Clark 1976; Söderström 2009; Yazama et al. 1997; Dym and Fawcett 1970). We found that the EC sheet remains tightly adhered to the MC sheet even after mechanical teasing with fine tweezers to isolate ST and remove connective tissue. Collagenase digestion was necessary to separate the two sheets that constitute the ST wall. The EC sheet is not an indifferent neighboring structure; it conforms to the ST surface during the process of contraction.

ET-1 treatment causes contraction of ST (Tripiciano et al. 1996). We observed by light and stereomicroscopy that ST diameter is ~40 % less under contracted versus relaxed condition (Fig. 1).

In relaxed ST, both MC and EC are flat polygonal cells. In our previous confocal microscopic study of tangential planes (Losinno et al. 2012), we found that MC in contracted ST have a smaller external area, greater height and a more rounded contour. The present study revealed that MC in contracted ST have a conical shape with the top pointing toward the tubule interior, based on light microscopy (Fig. 2b, d), TEM (Fig. 3b) and confocal microscopy (Fig. 6; Electronic Supplementary Material, Video S5). In confocal *z*-stack function of contracted ST immunostained with α-actin Ab, the deepest OS show isolated AF groups corresponding to the tops of cells, while the most superficial OS show the flat base of the cells, where AF form the peripheral belts and ribbons of the outer longitudinal layer (Fig. 6; Electronic Supplementary Material, Video S5).

EC adapt to the shape changes that MC undergo during contraction by increasing thickness, folding the nuclei and protruding the nuclei into the interstitium, as revealed by light

Author's personal copy

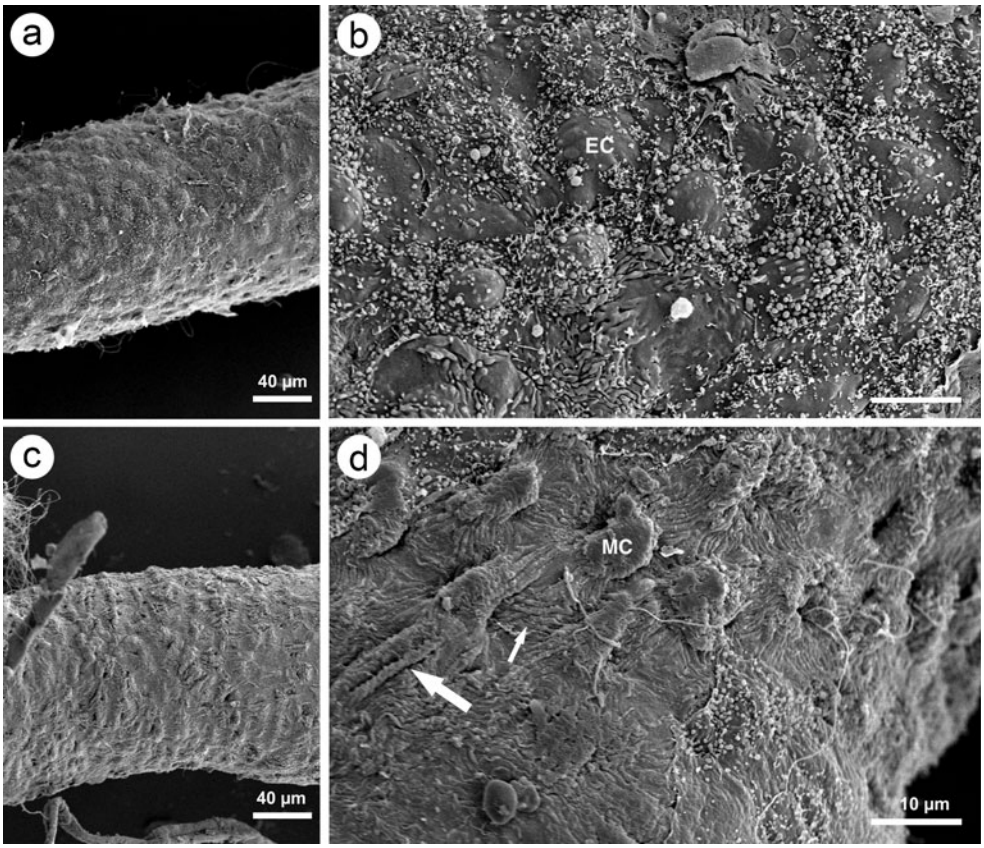

Fig. 9 SEM images of MC and EC monolayer surfaces in contracted ST. **a** Without digestion; EC monolayer is present. **b** Higher magnification of the ST segment in (**a**), showing numerous, variably-sized cytoplasmic projections of EC and protrusion of nuclei into the interstitium. *Bar* 10 μm. **c** The EC monolayer has been removed by digestion to reveal the MC monolayer. **d** Higher magnification of the ST segment in (**c**). MC have large folds (*large arrow*) parallel to the ST axis that cover the nuclei and small perpendicular folds (*small arrow*). A few remaining EC are present, revealed by their cytoplasmic projections

microscopy (Fig. 2d) and TEM (Fig. 4b). We propose a model for ST contraction in Fig. 10.

We were not able to measure the surface area of contracted EC by either confocal microscopy or SEM. The problem in confocal microscopy was that EC had no peripheral belt of AF to indicate the cell contour. The problem in SEM was that cell boundaries were obscured by the numerous cytoplasmic projections.

SEM examination of the MC surface requires removal of the EC sheet that externally covers the MC sheet. Collagenase digestion was performed in previous studies to remove the connective tissue of the interstitium (Maekawa et al. 1994,

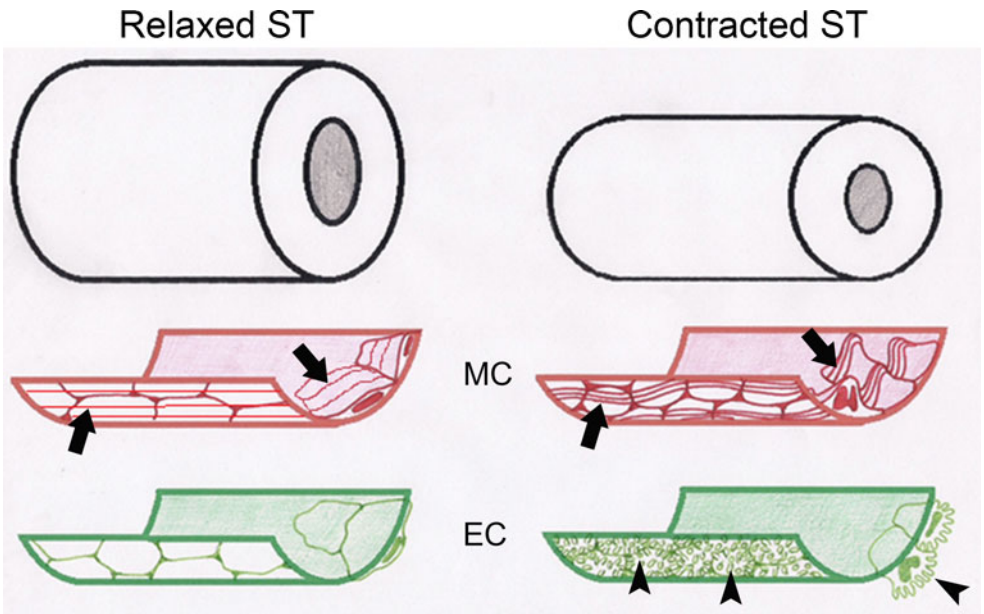

Fig. 10 Model for the ST contraction. Relaxed and contracted ST are shown, surrounded by two concentric sheets in the rat: the MC (*red*) and EC monolayers (*green*). In the relaxed case, both MC and EC are flat and polygonal. In the contracted case, MC adopt a conic shape with their tops towards the tubular center and their rounded bases towards the external surface. Note the disposition of AF in MC in relaxed and contracted ST (*arrows*). EC in contracted ST show multiple cytoplasmic projections to the interstitium (*arrowheads*). Basement membranes and collagen fibers are not drawn

Author's personal copy

1996; Tripiciano et al. 1996, 1997, 1999) but the EC sheet remained intact. Murakami et al. (1979) performed digestion of relaxed ST to examine the MC surface by SEM. They used a digestion method more aggressive than ours, involving treatment with HCl and collagenase following fixation but patches of the MC were also exfoliated, so it was impossible to identify the MC surface. Our method involved mechanical isolation of ST and careful, controlled digestion of the EC sheet to expose the MC monolayer in relaxed and contracted ST. This approach allowed better preservation of the ultrastructure without MC detachment.

For standardization of the digestion method (see Electronic Supplementary Material, Digestion), we determined an optimal condition with collagenase (0.5 mg/ml) treatment of ST for 5 min at 37 °C with gentle shaking. We were able to regulate digestion conditions to remove EC but with less distortion of the MC monolayer morphology, controlling the moment at which this situation was reached using confocal microscopy (see Electronic Supplementary Material, Fig. S3, Videos S1–3). We detected MC by α-actin Ab fluorescence, because EC do not express this isoform and detected EC using β-actin Ab, because the level of this isoform is very low in MC. We achieved ST contraction after EC digestion and before sample fixation.

Digestion did not alter ST diameter and therefore did not induce contraction by itself, as shown by SEM of relaxed ST (Fig. 8a, c).

It is difficult to distinguish MC from EC by SEM in relaxed ST because the two types of cells have similar size, shape and surface relief (smooth) (Fig. 8). In contrast, in contracted ST, EC have numerous finger-like surface projections facing the interstitium, which are easily distinguished from the folds seen on MC (Fig. 9b, d). Such finger-like projections have been described previously in TEM and SEM studies of EC from pulmonary arteries and are considered a distinctive feature of the inner layer of blood vessels in many species (Smith et al. 1971).

SEM observation of MC, following removal of EC by digestion, reveals many folds with differing orientations. The large folds run parallel to the tubular axis, forming thick ribbons above the nuclei (Fig. 9d). These findings are consistent with confocal microscopic images of the outer longitudinal layer of AF (Fig. 5, Contracted ST).

Because cell surface folding in the ST wall is considered a hallmark of contraction induced by a variety of stimuli (Palombi et al. 1992; Tripiciano et al. 1996, 1997, 1999; Romano et al. 2005), it is important to note the distinctive changes that occur in the two cell types in the wall of contracted ST: MC have folds, mostly parallel to the tubular axis (Fig. 9d), whereas EC have numerous small, finger-like projections (Fig. 9b).

Use of optimal digestion conditions as described here for removal of the EC monolayer prior to SEM imaging of the MC layer surface will facilitate future studies of ST contraction.

Our previous study showed that AF in contracted MC are arranged in two independent layers: an inner circular layer and an outer longitudinal layer (Losinno et al. 2012). Contraction of myofilaments in the two layers cause them to overlap and appear as thick electron-dense bundles in TEM micrographs, concurrent with cytoplasmic and nuclear folding (Fig. 3b, d). Our present findings show that the two AF layers assume different shapes during contraction: the inner circular layer takes on a convex shape that protrude into the ST, whereas the outer longitudinal layer remains shaped as a single plane and may become more rigid (Fig. 3d). Consistent results were obtained from confocal *z*-stack function (Fig. 6; Electronic Supplementary Material, Video S5).

Based on the results of this work, we interpret that ST contraction is originated in MC and transferred to the epithelium, where the pressure propels luminal fluid to the rete testis. It is evident that the contraction generated in MC is also transferred to the EC sheet because these cells change their shapes. We observed that the contraction force is not transferred by direct contact of MC with EC or Sertoli cells of the tubular epithelium but indirectly through collagen fibers that adopt a new arrangement in the two adjacent spaces and produce folding of the basement membranes (Fig. 4d). Transfer of the MC contraction force thus depends on (1) a strong junction between MC (as reflected by the thickness of the AF peripheral belt at the adherens junctions; Fig. 6), (2) anchorage of cytoskeletal filaments to the plasma membrane (Fig. 4c) and (3) collagen fibers that transfer the force to the germinal epithelium and endothelium.

In conclusion, the MC cytoskeleton in ST is different from that of other smooth muscle cells, has two independent layers of AF arranged orthogonally within the cytoplasm and the two layers adopt differing shapes during ST contraction: the inner layer becomes convex and the outer layer keeps flat, making a cone with the top to the center of the tubule. This arrangement impacts other components of the ST wall, such as EC, the basement membranes and the extracellular matrix. In this way, the ST wall responds as a unit to external stimuli to propel the tubular contents to the rete testis.

Acknowledgments This study was supported by the following grants: 06 J391, J025 and 06 J442 from SECyTP, UNCuyo, Argentina. The authors thank Dr. Silvia A. Belmonte for her most helpful comments on this manuscript. We appreciate the skilled technical assistance of Ing. Norberto Domizio and Ing. Elisa Bocanegra with light and electron microscopy. The authors also thank Stephen Anderson for editing assistance with the manuscript.

Author contributions A.D.L. contributed to the study design, acquisition and analysis of data for light and confocal microscopy and preparation of the manuscript. V.S. contributed to data analysis and interpretation for scanning electron microscopy. M.E. and F.E. contributed to perform the immunolocalizations. L.A.L contributed to drafting and critical revision of the manuscript. A.M contributed to study design, acquisition and analysis of data for light and transmission electron microscopy and preparation of the manuscript. All authors revised the manuscript and have approved the final version.

Author's personal copy

References

Clark RV (1976) Three-dimensional organization of testicular interstitial tissue and lymphatic space in the rat. Anat Rec 184:203–25

Dym M, Fawcett DW (1970) The blood-testis barrier in the rat and the physiological compartmentation of the seminiferous epithelium. Biol Reprod 3:308–26

Fawcett DW, Heidger PM, Leak LV (1969) Lymph vascular system of the interstitial tissue of the testis as revealed by electron microscopy. J Reprod Fertil 19:109–19

Fernández D, Bertoldi MV, Gómez L et al (2008) Identification and characterization of myosin from rat testicular peritubular myoid cells. Biol Reprod 79:1210–8

Filippini A, Tripiciano A, Palombi F et al (1993) Rat testicular myoid cells respond to endothelin: characterization of binding and signal transduction pathway. Endocrinology 133:1789–96

Kormano M, Hovatta O (1972) Contractility and histochemistry of the myoid cell layer of the rat seminiferous tubules during postnatal development. Z Anat Entwicklungsgesch 137:239–48

Leeson CR, Forman DE (1981) Postnatal development and differentiation of contractile cells within the rabbit testis. J Anat 132:491–511

Leeson CR, Leeson TS (1963) The postnatal development and differentiation of the boundary tissue of the seminiferous tubule of the rat. Anat Rec 147:243–59

Losinno AD, Morales A, Fernández D, Lopez LA (2012) Peritubular myoid cells from rat seminiferous tubules contain actin and myosin filaments distributed in two independent layers. Biol Reprod 86(150):1–8

Maekawa M, Nagano T, Murakami T (1994) Comparison of actin-filament bundles in myoid cells and Sertoli cells of the rat, golden hamster and mouse. Cell Tissue Res 275:395–8

Maekawa M, Kamimura K, Nagano T (1996) Peritubular myoid cells in the testis: their structure and function. Arch Histol Cytol 59:1–13

Murakami M, Hamasaki M, Okita S, Abe J (1979) SEM surface morphology of the contractile cells in the rat seminiferous tubules. Experientia 35:1099–101

Nixon GF, Mignery GA, Somlyo AV (1994) Immunogold localization of inositol 1,4,5-trisphosphate receptors and characterization of ultrastructural features of the sarcoplasmic reticulum in phasic and tonic smooth muscle. J Muscle Res Cell Motil 15:682–700

Palombi F, Salanova M, Tarone G et al (1992) Distribution of beta 1 integrin subunit in rat seminiferous epithelium. Biol Reprod 47: 1173–82

Rasband W (1997-2006) ImageJ. US National Institut of Health. Bethesda (MD). Avaible from http://rsb.info.nih.gov/ij/

Reynolds ES (1963) The use of lead citrate at high pH as an electron-opaque stain in electron microscopy. J Cell Biol 17:208–12

Romano F, Tripiciano A, Muciaccia B et al (2005) The contractile phenotype of peritubular smooth muscle cells is locally controlled: possible implications in male fertility. Contraception 72:294–7

Ross MH (1967) The fine structure and development of the peritubular contractile cell component in the seminiferous tubules of the mouse. Am J Anat 121:523–57

Smith U, Ryan JW, Michie DD, Smith DS (1971) Endothelial projections as revealed by scanning electron microscopy. Science 173:925–7

Söderström K-O (2009) Scanning Electron microscopy of mechanically isolated seminiferous tubules of the Rat testis. Andrologia 13:155–160

Spurr AR (1969) A low-viscosity epoxy resin embedding medium for electron microscopy. J Ultrastruct Res 26:31–43

Tripiciano A, Filippini A, Giustiniani Q, Palombi F (1996) Direct visualization of rat peritubular myoid cell contraction in response to endothelin. Biol Reprod 55:25–31

Tripiciano A, Palombi F, Ziparo E, Filippini A (1997) Dual control of seminiferous tubule contractility mediated by ETA and ETB endothelin receptor subtypes. FASEB J 11:276–86

Tripiciano A, Peluso C, Morena AR et al (1999) Cyclic expression of endothelin-converting enzyme-1 mediates the functional regulation of seminiferous tubule contraction. J Cell Biol 145:1027–38

Tung PS, Fritz IB (1990) Characterization of rat testicular peritubular myoid cells in culture: alpha-smooth muscle isoactin is a specific differentiation marker. Biol Reprod 42:351–65

Virtanen I, Kallajoki M, Närvänen O et al (1986) Peritubular myoid cells of human and rat testis are smooth muscle cells that contain desmin-type intermediate filaments. Anat Rec 215:10–20

Vogl AW, Soucy LJ, Lew GJ (1985) Distribution of actin in isolated seminiferous epithelia and denuded tubule walls of the rat. Anat Rec 213:63–71

Yazama F, Esaki M, Sawada H (1997) Immunocytochemistry of extracellular matrix components in the rat seminiferous tubule: electron microscopic localization with improved methodology. Anat Rec 248:51–62